I&EC research
Industrial & Engineering Chemistry Research

pubs.acs.org/IECR
Article

Continuous-Flow Glycerolysis of Urea to Glycerol Carbonate: The Critical Role of Operating Pressure

Andrea Severini,[⊥] Biagio Anderlini,[⊥] Antonio Lezza, Marianna Burello, Nicola Porcelli, Marco Mazzali, Veronica D'Eusanio, Mirco Rivi, Claudio Fontanesi,* and Fabrizio Roncaglia*

Cite This: *Ind. Eng. Chem. Res.* 2025, 64, 18630−18639

Read Online

ACCESS | Metrics & More | Article Recommendations | Supporting Information

ABSTRACT: A combined theoretical and experimental study on the carbonylation of glycerol with urea has identified low operating pressure as a key parameter for process optimization. Based on these insights, an improved multiple-pass continuous-flow system was developed, enabling the solvent-free synthesis of glycerol carbonate (GC) with enhanced efficiency. The optimized process achieved a productivity of ∼130 g/day, delivering high purity (>95%), and an isolated yield of 80%, thereby demonstrating the viability of this approach for sustainable GC production.

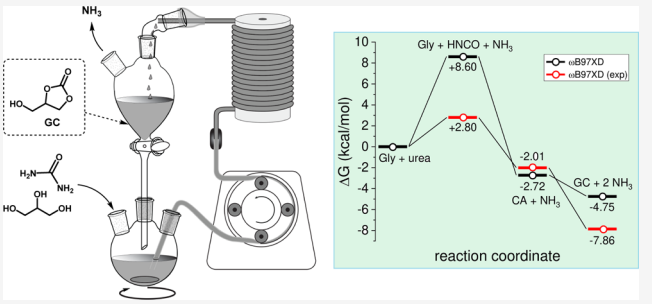

1. INTRODUCTION

Glycerol (Gly), a readily available byproduct of the rapidly expanding biodiesel industry, represents a crucial renewable feedstock for synthesizing valuable chemical building blocks.[1,2] Among these, glycerol carbonate (GC) holds a leading position due to its versatile chemical properties, making it a key intermediate for various applications, including solvents, electrolytes, and precursors for polymers and surfactants.[3]

Beyond its direct applications, GC's multisite electrophilic nature allows for efficient and selective interaction with diverse nucleophiles, facilitating its transformation into a wide array of valuable derivatives.[4−11] Notably, the free hydroxyl group of GC can be exploited directly or converted to generate new electrophilic sites.[12−15] GC also serves as a building block for various polymeric materials, including polyglycerols, polycarbonates, polyesters, acrylates, and isocyanate-free polyurethanes.[9,16−35] Furthermore, GC can function as a carbonate carrier in transcarbonylation processes with other polyols.[36,37] Importantly, the carbonate functional group of GC can be readily transformed into the highly electrophilic and valuable epoxy function.[38,39]

Several methods have been developed for the synthesis of GC from Gly. While direct carbonylation with CO_2 offers superior atom economy, it often suffers from low yields and poor selectivity.[40] Transesterification with other carbonates is among the more effective alternatives; however, the need for an alkyl carbonate to produce another alkyl carbonate, combined with significantly lower atom economy,[41] makes this route less appealing.[42] As a result, the carbonylation of glycerol with urea (Figure 1) is currently considered one of the most efficient and straightforward methods, generating only ammonia (NH_3) as a byproduct.[43]

This method becomes particularly attractive if ammonia—employed here as a CO_2 carrier—is efficiently recycled. In this context, the outgoing NH_3 stream can be easily absorbed into anhydrous ethanol and subsequently converted into insoluble ammonium carbamate by cobubbling with gaseous CO_2, providing a simple and effective capture route (Figure S1). The resulting solid can be filtered with ease and reconverted to urea via a low-temperature, metal-catalyzed process,[44] thus establishing a closed-loop system for CO_2 fixation into GC. This approach represents a significant improvement over conventional CO_2 scrubbing with NH_3 and traditional urea synthesis, which typically require high temperatures and extended reaction times.[45,46]

Various implementations of urea glycerolysis have been reported, most of which employ Zn-based catalysts or other Lewis acidic catalysts. Efforts to enhance yield and selectivity have included specialized heating methods such as microwave irradiation,[47,48] catalyst engineering,[49−52] and advances in reactor and process design.[41] In line with this latter approach, we recently proposed a novel continuous-flow tubular reactor[53] specifically designed to provide optimal thermal control and to efficiently collect the coproduced NH_3 via a membrane vacuum pump. To accommodate the relatively slow kinetics of the reaction, a multiple-pass configuration was implemented, ensuring sufficient contact time between reactants while

Received: June 23, 2025
Revised: August 28, 2025
Accepted: September 2, 2025
Published: September 10, 2025

https://doi.org/10.1021/acs.iecr.5c02554
Ind. Eng. Chem. Res. 2025, 64, 18630−18639

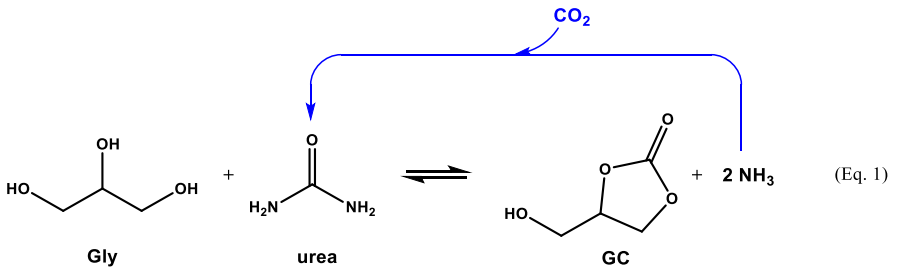

Figure 1. Gly carbonylation with urea to form GC.

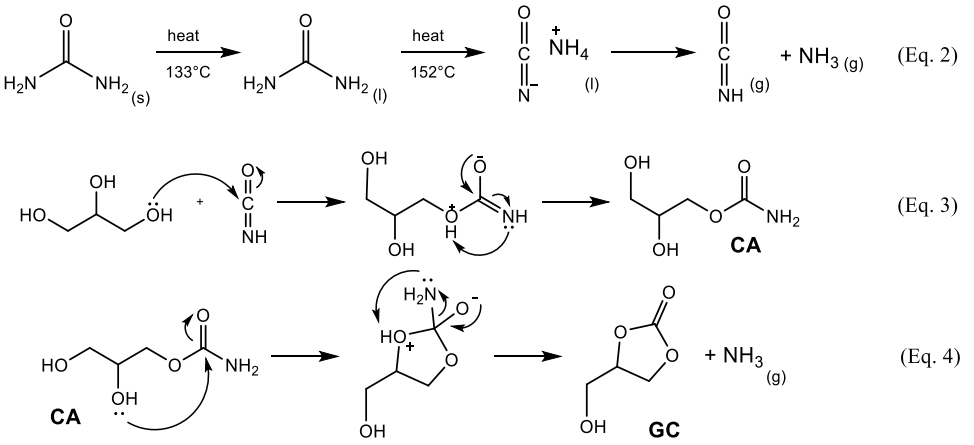

Figure 2. Possible steps followed by urea glycerolysis to GC.

maintaining compact system dimensions. In that study, three significant process parameters—temperature, reaction time, and the urea-to-Gly ratio—were investigated using a Design of Experiments (DoE) approach, leading to the identification of optimal operating ranges. However, the system faced technical challenges associated with pumping the initial urea/Gly mixture through the setup. To address this, preheating the mixture to 65 °C was employed, effectively reducing viscosity and improving solubility, thereby allowing reliable handling by the peristaltic pump. Nonetheless, this solution introduced a critical limitation: a minimum operating pressure of 400 mmHg, imposed by the mechanical sensitivity of the peristaltic tubing, which would shrink and deform at lower pressures. Consequently, despite its promising and scalable design, the system remained constrained by this pressure requirement—a factor believed to be a primary contributor to the modest yield achieved (approximately 42%). Notably, most of the higher-yielding urea glycerolysis processes reported in the recent literature operate under reduced pressure, often without providing detailed justification for this condition.

In the present study, a theoretical investigation was conducted to elucidate the reaction mechanism and assess the influence of the operating pressure on selectivity and yield. Computational results revealed a clear thermodynamic advantage to operating under reduced pressure, which prompted the development of an improved multipass continuous-flow system, enabling solvent-free synthesis of GC with significantly enhanced efficiency.

2. THEORETICAL CALCULATIONS

2.1. Calculation Details. The Gibbs free energy of GC formation was calculated using ab initio quantum mechanical based methods. Thermodynamic quantities were calculated following full geometry optimization and Hessian calculation.[54] All computations were carried out at the M06-2X and ωB97XD Density Functional Theory level of the theory, employing the 6-311G(d,p) basis set, chosen to accurately account for noncovalent interactions.[55] The close agreement between the results from both functionals confirmed the robustness of the model.

The reaction pathway was initially simulated in the gas phase as a simplified model. Solvent effects were then incorporated using the Integral Equation Formalism of the Polarizable Continuum Model (IEFPCM), parameterized with the dielectric constant (ε = 42.5) and refractive index (n = 2.172) of Gly. Comparison of gas phase and solvated calculations clearly demonstrated the profound influence of the solvent on both reaction energetics and pathway profiles (see Section 2.2.3). Notably, additional theoretical investigations were carried out as a function of temperature and pressure, enabling an assessment of their impact on the reaction mechanism. These insights proved to be valuable for guiding the optimization of the experimental setup. Full computational details, including input files, are provided in the Supporting Information.

2.2. Thermodynamic Analysis of GC Formation. *2.2.1. Mechanistic Considerations.* A literature review of Gly carbonylation with urea indicates that typical processes require temperatures greater than 150 °C and a Lewis acid catalyst, supporting the occurrence of a key reactive event: the thermal decomposition of urea into isocyanic acid (HNCO).[56] Urea alone is not sufficiently electrophilic to react directly with Gly; in contrast, isocyanic acid[3,42] and/or its metal complexes[43,46,57,58] are significantly more reactive. Thus, the initial step of the reaction is expected to involve the formation of one of these intermediates, as illustrated in Figure 2.

https://doi.org/10.1021/acs.iecr.5c02554
Ind. Eng. Chem. Res. 2025, 64, 18630−18639

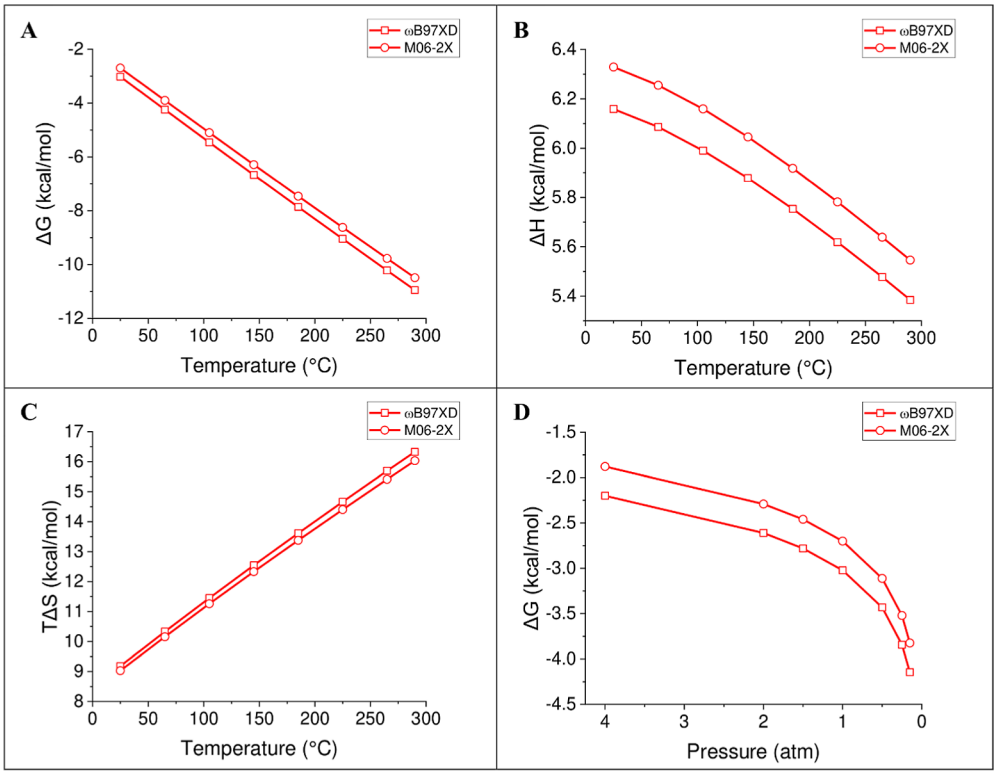

Figure 3. Calculated thermodynamic quantities for the GC formation reaction as a function of temperature and pressure. (A) Gibbs free energy of reaction as a function of temperature. (B) Reaction enthalpy as a function of temperature. (C) Reaction entropy as a function of temperature. (D) Gibbs free energy of the reaction as a function of pressure. All calculations are performed modeling Gly as the solvent using the IEFPCM.

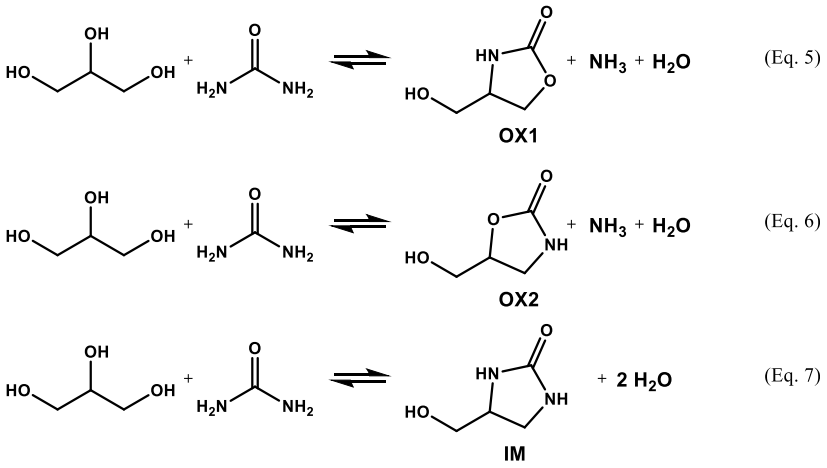

Figure 4. Possible side reaction pathways of urea glycerolysis.

The thermal behavior of urea (eq 2, Figure 2), thoroughly characterized by Schaber et al.,[56] involves its melting at 133 °C, followed by decomposition into HNCO and NH_3 at around 152 °C. This decomposition accelerates rapidly above 152 °C and proceeds via an ammonium cyanate intermediate. Furthermore, at temperatures above 190 °C, additional decomposition pathways occur, leading to the formation of secondary nitrogen-containing byproducts. These observations are consistent with our previous DoE evaluation,[53] which identified 185 °C as the most productive process temperature. Under these conditions, isocyanic acid/zinc isocyanate are expected to be the dominant electrophilic species reacting with Gly to form a linear carbamate intermediate (CA, eq 3, Figure 2). Subsequently (eq 4), an intramolecular nucleophilic attack of a hydroxyl oxygen on the carbamate carbonyl should proceed via a five-membered cyclic transition state, yielding GC and releasing a second molecule of NH_3.

2.2.2. Influence of Temperature and Pressure. The influence of operating variables on urea glycerolysis was assessed over the 25−290 °C range, the upper bound being limited by the boiling point of Gly. Thermodynamic parameters calculated under these conditions (Table S1) and in the solvated environment (Gly) revealed that GC formation becomes increasingly favorable with a rising temperature. As shown in Figure 3A, both M06-2X (square markers) and ωB97XD (circular markers) predict a progressive decrease in the ΔG of 7.79 and 7.93 kcal mol^{-1}, respectively. In addition, the reaction remains endothermic ($\Delta H > 0$) throughout the

https://doi.org/10.1021/acs.iecr.5c02554
Ind. Eng. Chem. Res. 2025, 64, 18630−18639

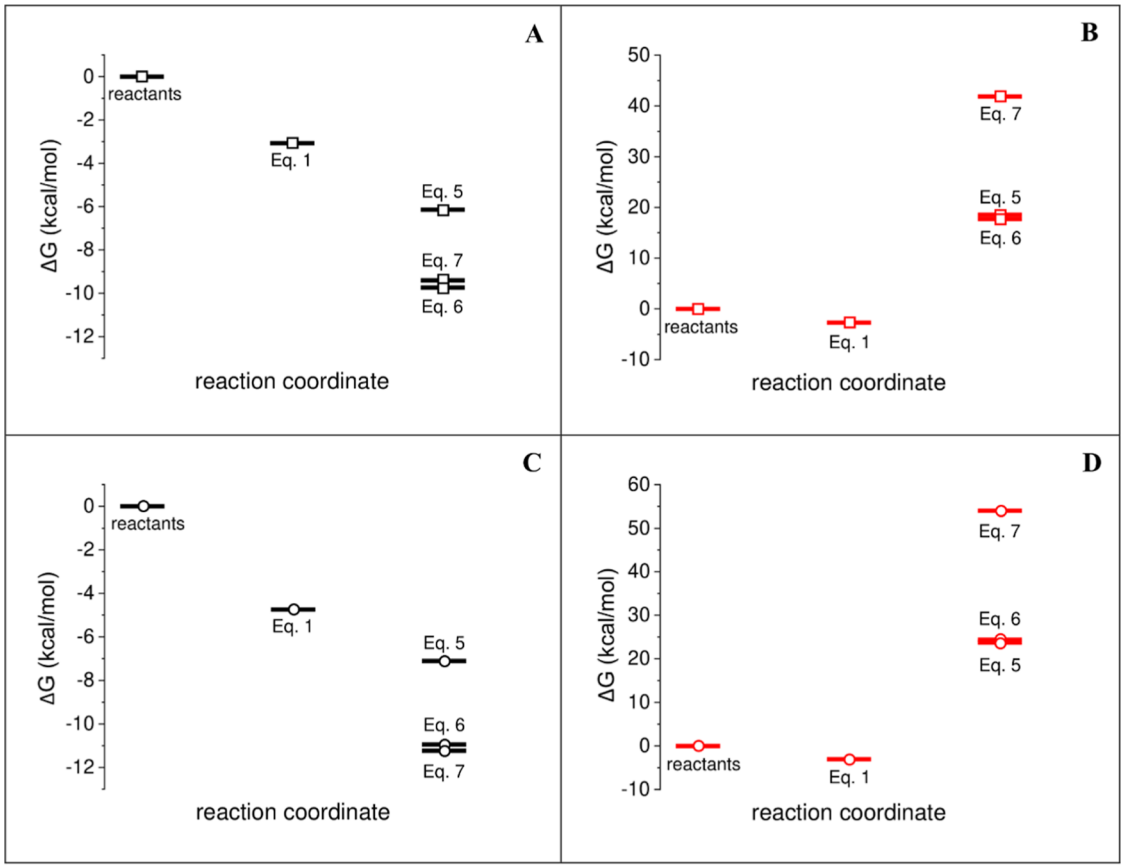

Figure 5. ΔG of the species illustrated in Figures 1 and 4. Calculations performed at the M06-2X level of theory (square markers) or performed at the ωB97XD level of theory (circular markers). (A,C) Calculation performed in the gas-phase (black markers). (B,D) Calculations performed in the solvated media (Gly) using the IEFPCM (red markers).

examined temperature range (Figure 3B), with negligible enthalpy change (0.78 kcal mol^{-1}), indicating that the temperature-driven gain in spontaneity is primarily entropic. In line with the Gibbs–Helmholtz relation ($\Delta G = \Delta H - T\Delta S$), both functionals predict a corresponding rise in $T\Delta S$ of ∼7 kcal mol^{-1} (Figure 3C), confirming entropy as the dominant driver at elevated temperatures.

Pressure dependence was also examined over 0.15 to 4.00 atm under the same solvation conditions (Figure 3D; Table S2). The lower limit of 0.15 atm corresponds to the practical achievable working vacuum inside the improved experimental plant (discussed later). Notably, ΔG decreases substantially under reduced pressure. This trend underscores both a thermodynamic benefit and a kinetic mass-action effect arising from the removal of gaseous NH_3 generated in urea decomposition (eq 2) and carbamate cyclization (eq 4), consistent with Le Chatelier's principle. Pressures below 0.15 atm would further enhance this driving force but may be constrained by urea sublimation losses.

Collectively, these results identify high temperature and reduced pressure as synergistic parameters that strongly favor GC formation through both thermodynamic and mass-action effects, thereby providing a solid theoretical rationale for the experimental process optimization.

2.2.3. Influence of Solvent. Across all computational scenarios—spanning different levels of theory and solvent conditions—the direct formation of GC was consistently predicted to be thermodynamically favored ($\Delta G < 0$; Figure 3A,D). Nonetheless, competing pathways leading to 2-oxazolidinones (OX1, OX2) and 2-imidazolidinone (IM) (Figure 4) cannot be excluded,[43,59,60] even though these species were not detected in our previous experimental studies.[53]

To address this discrepancy, we computed the thermodynamic parameters for these competing reactions (eqs 5, 6, and 7), benchmarking the relative stability of OX1, OX2, and IM against GC. Gas-phase calculations using both functionals consistently indicated that these byproducts are thermodynamically favored, as reflected by their negative ΔG values (Table S3), implying a preferential formation over GC under gas-phase conditions. This trend is also evidenced in Figure 5A (M06-2X functional) and Figure 5C (ωB97XD functional) using black markers.

Strikingly, inclusion of implicit solvation (IEFPCM, $\varepsilon = 42.5$ for Gly) reversed this trend. In fact, under solvated conditions (red markers), GC remained thermodynamically favorable, while the formation of OX1, OX2, and IM became strongly uphill. Specifically, ΔG values for OX1 and OX2 rose to ∼+18 kcal mol^{-1} (M06-2X) and ∼+24 kcal mol^{-1} (ωB97XD), whereas IM formation was even more disfavored, at ∼+42 kcal mol^{-1} (M06-2X) and ∼+54 kcal mol^{-1} (ωB97XD) (Figure 5B,D; Table S3).

This solvent-induced inversion underscores the pivotal role of the polar glycerol medium in dictating selectivity: by preferential stabilization of the reactants and transition states associated with GC formation, it suppresses competing pathways. This theoretical insight aligns seamlessly with our experimental observations, where GC was obtained with high

https://doi.org/10.1021/acs.iecr.5c02554
Ind. Eng. Chem. Res. 2025, 64, 18630−18639

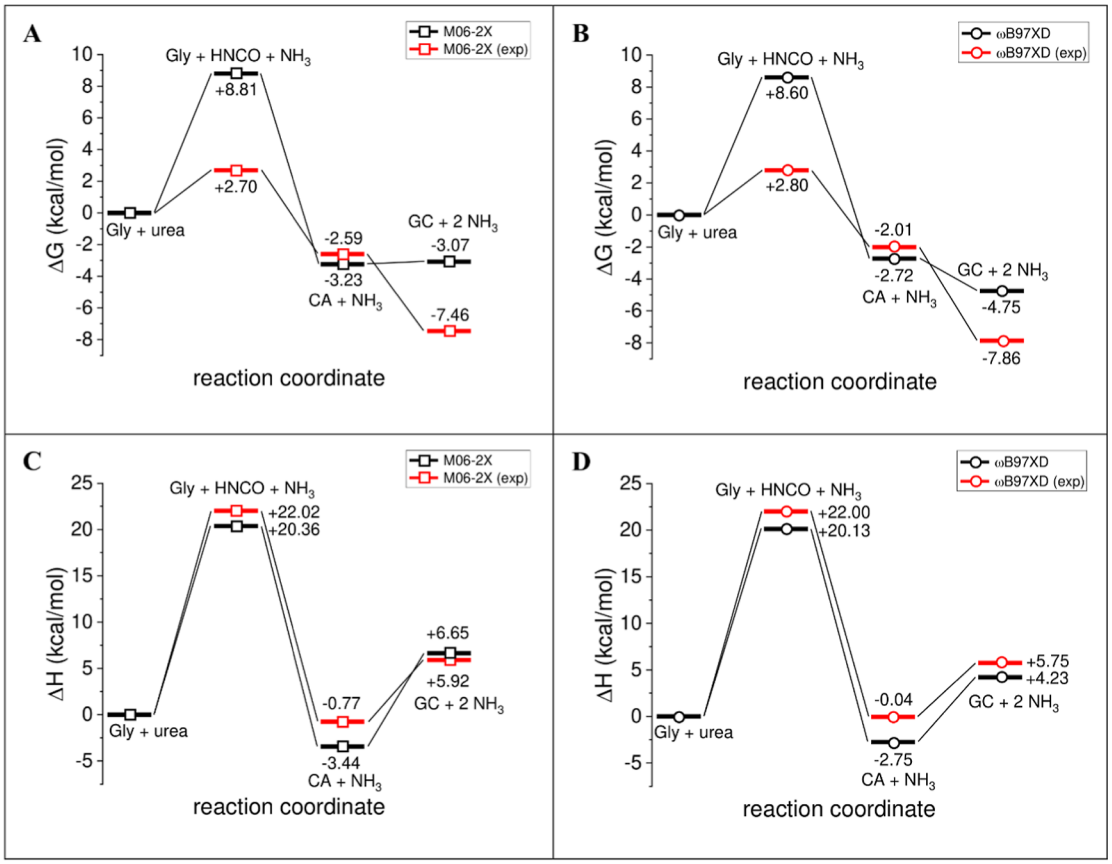

Figure 6. First row: PES versus reaction coordinates plot of the species illustrated in Figure 2. Second row: reaction enthalpy versus reaction coordinates of the species illustrated in Figure 2. Calculations performed at the M06-2X level of theory (square markers) or performed at the ωB97XD level of theory (circular markers). Calculations performed in the gas phase, T = 298 K and P = 1 atm (black curves) or performed in the solvated media (Gly), T = 458 K and P = 0.15 atm (red curves). To account for solvent effect, the IEFPCM was used.

selectivity, thus validating solvent effects as a key determinant of the reaction outcome.

The influence of other solvents on reaction selectivity was not explored because the solvent-free conditions—where glycerol serves as both reactant and solvent—offer significant operational advantages, particularly in terms of product recovery and process simplification. For instance, commonly used organic solvents have boiling points lower than the temperature required for urea thermolysis (T > 152 °C), while high-boiling solvents like dimethylformamide, *N*-methyl-2-pyrrolidinone, or dimethyl sulfoxide were not considered as they are toxic and/or difficult to remove at the end of the process. Moreover, other popular high-boiling solvents (e.g., ethylene glycol, propylene glycol) are incompatible as can produce unwanted side products.

2.2.4. Potential Energy Surface. The potential energy surfaces (PES) and enthalpy profiles for the transformations described in eqs 2 and 4 (Figure 2) were calculated under both gas-phase conditions (25 °C, 1 atm, no solvent; black curves) and optimized reaction conditions (185 °C, 0.15 atm, Gly as solvent; red curves). The first step—urea decomposition to isocyanic acid (eq 2)—was found to be thermodynamically unfavorable, with gas-phase calculations giving $\Delta G \approx$+8.7 kcal mol^{-1} (Figure 6A,B) and $\Delta H \approx$ +20.2 kcal mol^{-1} (Figure 6C,D). Under simulated reaction conditions (red curves), ΔG decreased modestly, while ΔH slightly increased, corroborating Schaber's experimental observations that this step is non-spontaneous and requires thermal activation.[56] The subsequent step, formation of CA from Gly and isocyanic acid (eq 3), was predicted to be both exergonic and exothermic, while the overall Gly-to-CA transformation (eqs 2 + 3) displayed only a modest thermodynamic driving force.

The final cyclization of CA to GC (eq 4) was consistently endothermic across all computational scenarios. Notably, its Gibbs free energy was markedly lowered under reaction conditions (Figure 6A,B), highlighting the entropic contribution to the process. These findings indicate that solvent stabilization combined with thermal and pressure effects is critical to bias the reaction toward GC formation.

Overall, the theoretical analysis establishes that elevated temperature (~185 °C), reduced pressure (~0.15 atm), and solvation in Gly collectively impose a pronounced entropic drive that favors GC formation, while solvation emerges as the key factor enforcing selectivity by destabilizing competing pathways. The transformation remains intrinsically endothermic (Figure 6C,D), with solvation imparting only minor enthalpic modulation. High temperature is indispensable not only to exploit this entropic contribution but also to enable the thermal decomposition of urea into isocyanic acid, the pivotal reactive intermediate.

3. EXPERIMENTAL SECTION

3.1. Materials and Methods. Unless otherwise stated, all solvents and reagents were of commercial grade and used as received. Vegetable-sourced glycerol (Gly), urea, and diethyl ether were purchased from Merck (Milano, Italy). Zinc sulfate

https://doi.org/10.1021/acs.iecr.5c02554
Ind. Eng. Chem. Res. 2025, 64, 18630−18639

heptahydrate ($ZnSO_4·7H_2O$), $CDCl_3$, and ethyl acetate were purchased form Carlo Erba reagents (Cornaredo (MI), Italy). 96% Sulfuric acid was purchased from AppliChem GmbH (Darmstadt, Germany).

Zinc sulfate monohydrate ($ZnSO_4·H_2O$) was prepared by heating $ZnSO_4·7H_2O$ at 130 °C overnight in an oven and subsequently stored in a desiccator. Gly was vacuum-dried (10 mmHg) for 4 h at 40 °C before use and stored in a capped bottle. Urea was dried at 65 °C overnight and stored in a desiccator.

^{1}H NMR spectra were acquired using a Bruker Avance 400 spectrometer (Billerica, MA, USA) using $CDCl_3$ as the solvent.

3.2. Continuous-Flow Reactor. The experimental plant assembly is depicted in Figure 7.

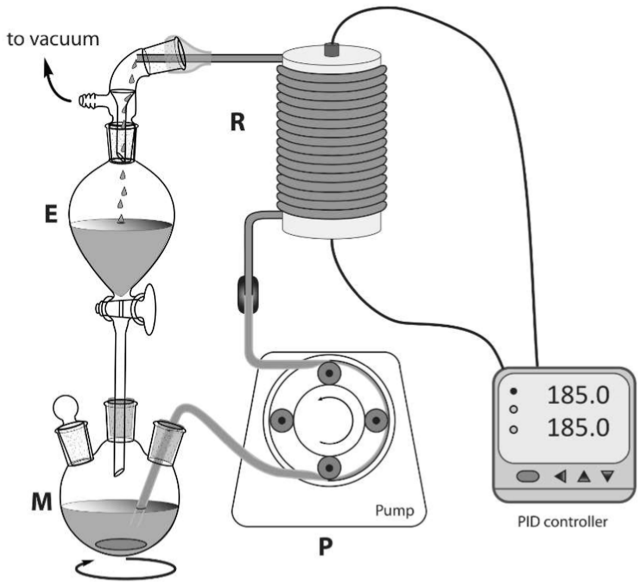

Figure 7. Layout of the continuous-flow reactor. M = mixing chamber; P = peristaltic pump; R = coiled tubular reactor; and E = expansion/collection chamber.

General description: in the mixing chamber (**M**), consisting of a three-necked round-bottom flask (25 mL for small scale and 100 mL for large scale), urea and $ZnSO_4·H_2O$ were dissolved in Gly and stirred via a standard stirring plate. The reaction mixture was pumped using a peristaltic pump (**P**, Bellco, model: BL 758, Mirandola, Italy) into a heated tubular reactor (**R**) and was then collected in a dropping funnel (E), where, keeping the tap closed, the desired vacuum level was set through a connection with a membrane vacuum pump. This flask serves as both a collecting container for GC and an expanding chamber to evacuate coproduced NH_3. The tubular AISI 316 stainless steel (1/16 in. OD × 1.2 mm ID, 3 m long, and ∼4 mL internal volume, obtained from Restek, Milano, Italy) reactor (**R**) was coiled around a 4 cm diameter cylindrical aluminum block. This block features dedicated slots for a heating resistor and a temperature sensor. These heating and measuring elements are connected to a PID controller (Rex-C100, obtained from RobotDigg, Shanghai, China), enabling precise temperature control. Thermal insulation was applied to the external surface of the reactor (not shown in the figure).

Process operation: unlike the earlier prototype,[53] the operativity of the plant was modified to make it compatible with pressures down to 25 mmHg (instead of 400 mmHg). The following changes were implemented:

- Peristaltic tubing was upgraded with a stiffer one, made of Tygon.
- The reaction mixture was prepared in **M** and pumped at rt. This operating temperature prevented the peristaltic tubing from softening due to heating.
- To ensure a homogeneous solution of urea in Gly at rt, the required urea amount was added in portions, processing each one at 185 °C and ∼150 mmHg through the reactor **R**, before the insertion of the subsequent portion (into **M**). This operating procedure resulted in fixation of urea as CA (eq 3, Figure 2), avoiding urea sublimation.
- After all the urea was added, the mixture was recirculated by opening the tap of **E**, and the process pressure was reduced to the optimal value as discussed later, to allow the conversion of CA into GC (eq 4).

3.3. Multiple-Pass Continuous-Flow Operation. The system operation consists of two stages as follows. In the first stage, urea was converted into CA, while evolving the first mole of NH_3. Once in this form, urea sublimation was avoided, enabling the free application of low pressures. The full urea amount was typically subdivided into six portions.

3.3.1. Small-Scale Operation. Gly (13.0 g; 0.141 mol, 1 equiv), urea (1.63 g; 0.027 mol, 0.2 equiv), and $ZnSO_4·H_2O$ (0.760 g; 4.2 mmol, 3 mol % relative to urea) were first added into a 25 mL mixing chamber (**M**, Figure 7) and stirred at rt until a homogeneous mixture was obtained. In the meantime, **R** temperature and pressure were set at the desired values, typically 185 °C and 150 mmHg, respectively. The mixture was then pumped at 1.2 mL/min through **R** and collected into **E** (tap closed). Afterward, the vacuum was temporarily disengaged, and the funnel tap was opened to allow the mixture to flow back into **M**. At this point, the following portion of urea (1.63 g, 0.027 mol, 0.2 equiv) was added, and the mixture was reprocessed as previously described. This procedure was repeated until the full amount of urea (9.74 g, 0.162 mol, 1.15 equiv) had been introduced and reacted.

In the second stage, the mixture obtained in the first stage was passed three times through the reactor **R**, set at 185 °C and 150 mmHg, maintaining the flow at 1.2 mL/min. The entire process involved nine passes through the tubular reactor, each pass taking approximately 16 min, resulting in an overall reaction time of 2 h and 25 min.

Workup. To remove the residual polar fraction, the crude was treated at 120 °C and 200 mmHg, until boiling ceased (∼2 h). Afterward, H_2O (0.1 mL per gram of crude) was added and the mixture extracted with EtOAc/Et_2O (4:1$_{v/v}$, 3 × 1.67 mL per gram of crude). Evacuation at reduced pressure yielded a purified product, composed of GC (>95% ^{1}H NMR purity) and minor amounts of DGTC, in 80% yield.

3.3.2. Larger Scale Operation. Gly (48.0 g; 0.52 mol, 1 equiv), urea (6.00 g; 0.10 mol, 0.2 equiv), and $ZnSO_4·H_2O$ (3.22 g; 18 mmol, 3 mol % relative to urea) were first added into a 100 mL mixing chamber (**M**, Figure 7) and stirred at rt until a homogeneous mixture was obtained. In the meantime, **R** temperature and pressure were set at the desired values, typically 185 °C and 150 mmHg, respectively. The mixture was then pumped at 1.2 mL/min through **R** and collected into **E** (tap closed). Afterward, vacuum was temporarily disengaged, and the funnel tap was opened to allow the mixture to flow

https://doi.org/10.1021/acs.iecr.5c02554
Ind. Eng. Chem. Res. 2025, 64, 18630−18639

back into **M**. At this point, the following portion of urea (6.00 g, 0.10 mol, 0.2 equiv) was added, and the mixture was reprocessed as previously described. This procedure was repeated until the full amount of urea (36.0 g, 0.60 mol, 1.15 equiv) had been introduced and reacted.

In the second stage, the mixture obtained in the first stage was passed three times through the reactor **R**, set at 185 °C and 150 mmHg, maintaining the flow at 1.2 mL/min. The entire process involved nine passes through the tubular reactor, each pass taking approximately 1 h, resulting in an overall reaction time of 9 h.

Workup. To remove the residual polar fraction, the crude was treated at 120 °C and 200 mmHg, until boiling ceased (~2 h). Afterward, H_2O (0.1 mL per gram of crude) was added and the mixture extracted with EtOAc/Et_2O ($4{:}1_{v/v}$, 3 × 1.67 mL per gram of crude). Evacuation at reduced pressure yielded a purified product (49.15 g), composed of GC (>95% ^{1}H NMR purity) and minor amounts of DGTC, in 80% yield.

3.3.3. Hydrolysis of GC/DGTC Mixture to Pure GC. To convert the residual DGTC into CG, a controlled hydrolysis process was set up as follows: Inside a round-bottom flask of suitable volume, the GC/DGTC mixture was mixed with H_2SO_4 (0.5 mL of a 1% aqueous solution per gram of GC/DGTC mixture), and the resulting solution was heated at 60 °C for 1 h 30 min. The product was extracted with EtOAc (1.5 mL per gram of initial mixture) and washed with water (3 × (0.5 mL per gram of initial mixture)), and the product was obtained after removal of organic solvent, yielding DGTC-free GC as a colorless oil, and ~90% yield.

4. RESULTS AND DISCUSSION

To extend the operating pressure range below 400 mmHg,[53] urea was added in portions to obtain a homogeneous solution in Gly at rt. This strategy circumvented thermal softening of the peristaltic tubing under reduced pressures (see the Experimental Section). A preliminary evaluation using the standard urea/Gly molar ratio of 1.15 [53] revealed that splitting urea into six added aliquots was required to fully dissolve urea at 25 °C, while division into four equal portions resulted in incomplete solubilization and subsequent pump clogging. Consequently, partitioning urea into six equal portions was adopted as the standard protocol. It was also observed that urea solubility improves over time, suggesting a better solubility into CA, compared to that in Gly.

Further preliminary experiments aimed to validate key theoretical insights, particularly the role of urea thermolysis to isocyanic acid as a prerequisite for glycerolysis, were conducted. Reactions conducted below 130 °C, regardless of $ZnSO_4{\cdot}H_2O$ catalyst presence, pressure, or duration, yielded no detectable Gly conversion. These results provide strong evidence that urea thermolysis is essential for reaction initiation. Partial Gly conversion was first observed at 150 °C, implicating HNCO as the key electrophile in the process. At this temperature and under the lowest attainable working pressure (25 mmHg), a GC yield of 50% was obtained, though urea sublimation partially compromised mass balance. Based on these findings, the process temperature was fixed at 185 °C, and a systematic evaluation of other operating variables was conducted (Table 1).

Operating under reduced pressure significantly enhanced reaction performance, as observed in entries 1−5 of Table 1. In agreement with the theoretical model, lower operating pressures are expected to accelerate CA cyclization to GC (eq 4). However, yields plateaued between 110 mmHg (entry 5) and 150 mmHg (entry 4), establishing 150 mmHg as the optimal pressure. Overall, reduced pressures improved both the yield and selectivity. In contrast, higher pressures (entries 1 and 2) favored the formation of a secondary product, identified as diglycerol tricarbonate (DGTC, Figure 8), as confirmed by ^{1}H NMR spectroscopy.

Table 1. Urea Glycerolysis Conducted in Flow, within the Experimental Setup of Figure 7[a]

experiment no.	urea/Gly molar ratio	no of urea portions	*T* (°C)	*P* (mmHg)	yield (%)
1	1.15	6	185	400	44
2	1.15	6	185	300	55
3	1.15	6	185	200	72
4	1.15	6	185	150	80
5	1.15	6	185	110	80
6	1.80	8	185	150	80
7	1.10	6	185	150	76
8	1.05	6	185	150	69
9[b]	1.15	6	185	150	80
10[b]	1.15	6	185	110	80
11[c]	1.15	6	185	150	15
12	1.15	6	170	150	59

[a]Common conditions: 185 °C, multiple pass (see the Experimental Section), Gly (13.0 g; 0.141 mol), urea (amount according to Table), $ZnSO_4{\cdot}H_2O$ (0.760 g; 4.2 mmol), and flow: 1.2 mL/min. [b]Gly (48.0 g; 0.52 mol), urea (36.0 g, 0.60 mol), $ZnSO_4{\cdot}H_2O$ (3.22 g; 18 mmol). [c]$ZnSO_4{\cdot}H_2O$ was omitted.

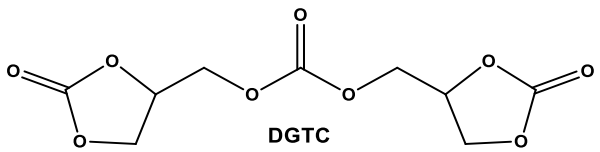

Figure 8. Structure of diglycerol tricarbonate (DGTC).

To recover GC from GC/DGTC mixtures, a mild acid hydrolysis protocol was developed, exploiting the higher stability of cyclic carbonates compared to the central linkage of DGTC (see the Experimental Section). Notably, DGTC formation decreased with decreasing pressure, suggesting that DGTC likely forms through an interaction between GC and unconverted CA—a side pathway that is suppressed when NH_3 is rapidly removed under vacuum, allowing efficient CA conversion.

The effect of urea/Gly molar ratio was also evaluated (entries 4 and 6−8, Table 1), confirming 1.15 as the optimal value, in agreement with previous investigations.[53] Lower ratios (1.10 or 1.05) resulted in decreased yields, while increasing the ratio offered no advantage.

The process demonstrated strong robustness upon scale-up (entries 9 and 10), with minimal differences observed when the pressure was reduced from 150 to 110 mmHg. Catalyst omission (entry 11) resulted in a marked performance decline, corroborating its essential role in facilitating urea thermolysis. Furthermore, the benefit of operating at 185 °C was reinforced through a comparison to a run at 170 °C (entry 12), which resulted in substantially lower GC yields.

The solvent-free nature of the process (i.e., absence of volatile cosolvents) enables low-pressure operation, facilitating continuous NH_3 removal and DGTC minimization. As a result,

https://doi.org/10.1021/acs.iecr.5c02554
Ind. Eng. Chem. Res. 2025, 64, 18630−18639

high product purity (>95%, Figure S2) was achieved, exceeding that of several commercial sources.

The multiple-pass continuous-flow system (Figure 7) provided excellent process control, as demonstrated at the scale by converting 48 g of Gly into 49 g of GC over 9 h of operation. This corresponds to a daily throughput of ∼130 g of high-purity GC, requiring only minimal amounts of organic solvent during workup. The production scale can also be readily increased by employing longer tubular reactors to accommodate higher flow rates while maintaining residence time and thermal profiles.

5. CONCLUSIONS

Theoretical thermodynamic calculations provided valuable mechanistic insights into the urea glycerolysis toward GC; most of them were experimentally validated. Elevated temperatures were shown to impart a strong entropic driving force (Figure 3A,C) and provide the necessary thermal activation for urea thermolysis into isocyanic acid. Additionally, reduced operating pressures contributed both a thermodynamic push (Figure 3D) and mass-action-driven ammonia removal, able to accelerate the conversion of CA into GC. The glycerol medium (i.e., solventless conditions) further proved pivotal in suppressing byproduct formation through solvent stabilization effects.

The implementation of the theoretical indications within the experimental setup led to a substantial improvement in both yield and selectivity compared with our previous setup. The optimized solvent-free process delivered high-purity GC in an 80% isolated yield with minimal downstream processing. The product purity can be further upgraded via the controlled hydrolysis of the main byproduct, DGTC, reaching purity levels exceeding some commercial offerings. Scale-up under optimal conditions (185 °C, 150 mmHg) achieved a daily production of ∼130 g of GC without any loss in yield or quality, demonstrating the robustness, efficiency, and scalability of this multiple-pass continuous-flow approach toward GC.

■ ASSOCIATED CONTENT

Supporting Information

The Supporting Information is available free of charge at https://pubs.acs.org/doi/10.1021/acs.iecr.5c02554.

Sketch of the experimental CO_2−NH_3 scrubber/adsorber; ^{1}H NMR spectrum of GC obtained according to procedure 3.3.2.; details of theoretical calculation (Gaussian input files) and tabulated thermodynamic parameters, including their variation with temperature; ΔG dependence on pressure; and ΔG of formation for possible byproducts (PDF)

■ AUTHOR INFORMATION

Corresponding Authors

Fabrizio Roncaglia − *Department of Chemical and Geological Sciences, (DSCG), University of Modena and Reggio Emilia, Modena 41125, Italy; National Interuniversity Consortium of Materials Science and Technology (INSTM), Firenze 50121, Italy; Interdepartmental Centre H2-MORE, University of Modena and Reggio Emilia, Modena 41125, Italy;* orcid.org/0000-0001-7630-4375; Email: fabrizio.roncaglia@unimore.it

Claudio Fontanesi − *Department of Engineering "Enzo Ferrari", (DIEF), University of Modena and Reggio Emilia, Modena 41125, Italy; National Interuniversity Consortium of Materials Science and Technology (INSTM), Firenze 50121, Italy;* orcid.org/0000-0002-1183-2406; Email: claudio.fontanesi@unimore.it

Authors

Andrea Severini − *Department of Chemical and Geological Sciences, (DSCG), University of Modena and Reggio Emilia, Modena 41125, Italy*

Biagio Anderlini − *Department of Chemical and Geological Sciences, (DSCG), University of Modena and Reggio Emilia, Modena 41125, Italy;* orcid.org/0000-0003-4641-3137

Antonio Lezza − *Department of Chemical and Geological Sciences, (DSCG), University of Modena and Reggio Emilia, Modena 41125, Italy;* orcid.org/0009-0007-6773-7081

Marianna Burello − *Department of Chemical and Geological Sciences, (DSCG), University of Modena and Reggio Emilia, Modena 41125, Italy; National Interuniversity Consortium of Materials Science and Technology (INSTM), Firenze 50121, Italy*

Nicola Porcelli − *Department of Chemical and Geological Sciences, (DSCG), University of Modena and Reggio Emilia, Modena 41125, Italy*

Marco Mazzali − *Department of Chemical and Geological Sciences, (DSCG), University of Modena and Reggio Emilia, Modena 41125, Italy*

Veronica D'Eusanio − *Department of Chemical and Geological Sciences, (DSCG), University of Modena and Reggio Emilia, Modena 41125, Italy; National Interuniversity Consortium of Materials Science and Technology (INSTM), Firenze 50121, Italy*

Mirco Rivi − *Department of Chemical and Geological Sciences, (DSCG), University of Modena and Reggio Emilia, Modena 41125, Italy; National Interuniversity Consortium of Materials Science and Technology (INSTM), Firenze 50121, Italy*

Complete contact information is available at: https://pubs.acs.org/10.1021/acs.iecr.5c02554

Author Contributions

$^{\perp}$A.S. and B.A. contributed equally to this work.

Notes

The authors declare no competing financial interest.

■ REFERENCES

(1) Naik, S. N.; Goud, V. V.; Rout, P. K.; Dalai, A. K. Production of First and Second Generation Biofuels: A Comprehensive Review. *Renew. Sustain. Energy Rev.* **2010**, *14* (2), 578−597.

(2) Zhou, C.-H.; Beltramini, J. N.; Fan, Y. X.; Lu, G. Q. M. Chemoselective Catalytic Conversion of Glycerol as a Biorenewable Source to Valuable Commodity Chemicals. *Chem. Soc. Rev.* **2008**, *37* (3), 527−549.

(3) Sonnati, M. O.; Amigoni, S.; Taffin De Givenchy, E. P.; Darmanin, T.; Choulet, O.; Guittard, F. Glycerol Carbonate as a Versatile Building Block for Tomorrow: Synthesis, Reactivity, Properties and Applications. *Green Chem.* **2013**, *15* (2), 283−306.

(4) Selva, M.; Fabris, M. The Reaction of Glycerol Carbonate with Primary Aromatic Amines in the Presence of Y- and X-Faujasites: The Synthesis of N-(2,3-Dihydroxy)Propyl Anilines and the Reaction Mechanism. *Green Chem.* **2009**, *11* (8), 1161−1172.

(5) Nohra, B.; Candy, L.; Blanco, J.; Raoul, Y.; Mouloungui, Z. Synthesis of Five and Six-Membered Cyclic Glycerilic Carbonates

Bearing Exocyclic Urethane Functions. *Eur. J. Lipid Sci. Technol.* **2012**, *115* (1), 111−122.
(6) Fricke, N.; Keul, H.; Möller, M. Carbonate Couplers and Functional Cyclic Carbonates from Amino Acids and Glucosamine. *Macromol. Chem. Phys.* **2009**, *210* (3−4), 242−255.
(7) Bao, Y.-M.; Shen, G.-R.; He, J.; Li, Y.-S. Water-Soluble Hyperbranched Poly(Ester Urethane)s Based on d,l-Alanine: Isocyanate-Free Synthesis, Post-Functionalization and Application. *Green Chem.* **2012**, *14* (8), 2243.
(8) Galletti, G.; Prete, P.; Vanzini, S.; Cucciniello, R.; Fasolini, A.; De Maron, J.; Cavani, F.; Tabanelli, T. Glycerol Carbonate asaVersatile Alkylating Agent fortheSynthesis of *β*-Aryloxy Alcohols. *ACS Sustain. Chem. Eng.* **2022**, *10* (33), 10922−10933.
(9) Ghandi, M.; Mostashari, A.; Karegar, M.; Barzegar, M. Efficient Synthesis of A-Monoglycerides via Solventless Condensation of Fatty Acids with Glycerol Carbonate. *J. Amer Oil Chem. Soc.* **2007**, *84*, 681−685.
(10) Simão, A.-C.; Lynikaite-Pukleviciene, B.; Rousseau, C.; Tatibouët, A.; Cassel, S. 1,2-Glycerol Carbonate: A Versatile Renewable Synthon. *Lett. Org. Chem.* **2006**, *3*, 744.
(11) Quienne, B.; Poli, R.; Pinaud, J.; Caillol, S. Enhanced Aminolysis of Cyclic Carbonates by *β*-Hydroxylamines for the Production of Fully Biobased Polyhydroxyurethanes. *Green Chem.* **2021**, *23* (4), 1678−1690.
(12) Da Costa, P. L. F.; Melo, V. N.; Guimarães, B. M.; Schuler, M.; Pimenta, V.; Rollin, P.; Tatibouët, A.; De Oliveira, R. N. Glycerol Carbonate in Ferrier Reaction: Access to New Enantiopure Building Blocks to Develop Glycoglycerolipid Analogues. *Carbohydr. Res.* **2016**, *436*, 1−10.
(13) Carré, C.; Zoccheddu, H.; Delalande, S.; Pichon, P.; Avérous, L. Synthesis and Characterization of Advanced Biobased Thermoplastic Nonisocyanate Polyurethanes, with Controlled Aromatic-Aliphatic Architectures. *Eur. Polym. J.* **2016**, *84*, 759−769.
(14) Rousseau, J.; Rousseau, C.; Lynikaitė, B.; Šačkus, A.; De Leon, C.; Rollin, P.; Tatibouët, A. Tosylated Glycerol Carbonate, a Versatile Bis-Electrophile to Access New Functionalized Glycidol Derivatives. *Tetrahedron* **2009**, *65* (41), 8571−8581.
(15) Legros, V.; Taing, G.; Buisson, P.; Schuler, M.; Bostyn, S.; Rousseau, J.; Sinturel, C.; Tatibouët, A. Activated Glycerol Carbonates, Versatile Reagents with Aliphatic Amines: Formation and Reactivity of Glycidyl Carbamates and Trialkylamines. *Eur. J. Org Chem.* **2017**, *2017* (34), 5032−5043.
(16) Quienne, B.; Kasmi, N.; Dieden, R.; Caillol, S.; Habibi, Y. Isocyanate-Free Fully Biobased Star Polyester-Urethanes: Synthesis and Thermal Properties. *Biomacromolecules* **2020**, *21* (5), 1943−1951.
(17) Parzuchowski, P. G.; Świderska, A.; Roguszewska, M.; Frączkowski, T.; Tryznowski, M. Amine Functionalized Polyglycerols Obtained by Copolymerization of Cyclic Carbonate Monomers. *Polymer* **2018**, *151*, 250−260.
(18) Rokicki, G.; Rakoczy, P.; Parzuchowski, P.; Sobiecki, M. Hyperbranched Aliphatic Polyethers Obtained from Environmentally Benign Monomer: Glycerol Carbonate. *Green Chem.* **2005**, *7* (7), 529.
(19) Vogt, L.; Ruther, F.; Salehi, S.; Boccaccini, A. R. Poly(Glycerol Sebacate) in Biomedical Applications—A Review of the Recent Literature. *Adv. Healthc. Mater.* **2021**, *10* (9), 2002026.
(20) Zhang, H.; Grinstaff, M. W. Recent Advances in Glycerol Polymers: Chemistry and Biomedical Applications. *Macromol. Rapid Commun.* **2014**, *35* (22), 1906−1924.
(21) Ekladious, I.; Liu, R.; Zhang, H.; Foil, D. H.; Todd, D. A.; Graf, T. N.; Padera, R. F.; Oberlies, N. H.; Colson, Y. L.; Grinstaff, M. W. Synthesis of Poly(1,2-Glycerol Carbonate)−Paclitaxel Conjugates and Their Utility as a Single High-Dose Replacement for Multi-Dose Treatment Regimens in Peritoneal Cancer. *Chem. Sci.* **2017**, *8* (12), 8443−8450.
(22) Kundys, A.; Plichta, A.; Florjańczyk, Z.; Zychewicz, A.; Lisowska, P.; Parzuchowski, P.; Wawrzyńska, E. Multi-Arm Star Polymers of Lactide Obtained in Melt in the Presence of Hyperbranched Oligoglycerols. *Polym. Int.* **2016**, *65*, 927−937.
(23) Mamiński, M. Ł.; Czarzasta, M.; Parzuchowski, P. Wood Adhesives Derived from Hyperbranched Polyglycerol Cross-Linked with Hexamethoxymethyl Melamines. *Int. J. Adhes. Adhes.* **2011**, *31* (7), 704−707.
(24) Jansen, J. F. G. A.; Dias, A. A.; Dorschu, M.; Coussens, B. Fast Monomers: Factors Affecting the Inherent Reactivity of Acrylate Monomers in Photoinitiated Acrylate Polymerization. *Macromolecules* **2003**, *36* (11), 3861−3873.
(25) Mhanna, A.; Sadaka, F.; Boni, G.; Brachais, C.; Brachais, L.; Couvercelle, J.; Plasseraud, L.; Lecamp, L. Photopolymerizable Synthons from Glycerol Derivatives. *J. Am. Oil Chem. Soc.* **2014**, *91* (2), 337−348.
(26) Ibn El Alami, M. S.; Suisse, I.; Fadlallah, S.; Sauthier, M.; Visseaux, M. Telomerization of 1,3-Butadiene with Glycerol Carbonate and Subsequent Ring-Opening Lactone Co-Polymerization. *Comptes Rendus Chim* **2016**, *19* (3), 299−305.
(27) Wu, Z.; Tang, L.; Dai, J.; Qu, J. Synthesis and Properties of Aqueous Cyclic Carbonate Dispersion and Non-Isocyanate Polyurethanes under Atmospheric Pressure. *Prog. Org. Coat.* **2019**, *136*, 105209.
(28) Ke, J.; Li, X.; Jiang, S.; Liang, C.; Wang, J.; Kang, M.; Li, Q.; Zhao, Y. Promising Approaches to Improve the Performances of Hybrid Non-Isocyanate Polyurethane. *Polym. Int.* **2019**, *68*, 651−660.
(29) Annunziata, L.; Diallo, A. K.; Fouquay, S.; Michaud, G.; Simon, F.; Brusson, J.-M.; Carpentier, J.-F.; Guillaume, S. M. *α,ω*-Di(Glycerol Carbonate) Telechelic Polyesters and Polyolefins as Precursors to Polyhydroxyurethanes: An Isocyanate-Free Approach. *Green Chem.* **2014**, *16* (4), 1947−1956.
(30) Duval, C.; Kébir, N.; Jauseau, R.; Burel, F. Organocatalytic Synthesis of Novel Renewable Non-isocyanate Polyhydroxyurethanes. *J. Polym. Sci. Part Polym. Chem.* **2016**, *54* (6), 758−764.
(31) Ekin, A.; Webster, D. C. Synthesis and Characterization of Novel Hydroxyalkyl Carbamate and Dihydroxyalkyl Carbamate Terminated Poly(Dimethylsiloxane) Oligomers and Their Block Copolymers with Poly(*ε*-Caprolactone). *Macromolecules* **2006**, *39* (25), 8659−8668.
(32) Tachibana, Y.; Shi, X.; Graiver, D.; Narayan, R. The Use of Glycerol Carbonate in the Preparation of Highly Branched Siloxy Polymers. *Silicon* **2015**, *7* (1), 5−13.
(33) Nomanbhay, S.; Ong, M. Y.; Chew, K. W.; Show, P.-L.; Lam, M. K.; Chen, W.-H. Organic Carbonate Production Utilizing Crude Glycerol Derived as By-Product of Biodiesel Production: A Review. *Energies* **2020**, *13* (6), 1483.
(34) Sacripante, G. G.; Zhou, K.; Farooque, M. Sustainable Polyester Resins Derived from Rosins. *Macromolecules* **2015**, *48* (19), 6876−6881.
(35) Magniont, C.; Escadeillas, G.; Oms-Multon, C.; De Caro, P. The Benefits of Incorporating Glycerol Carbonate into an Innovative Pozzolanic Matrix. *Cem. Concr. Res.* **2010**, *40* (7), 1072−1080.
(36) Hough, L.; Priddle, J. E.; Theobald, R. S. 363. Carbohydrate Carbonates. Part II. Their Preparation by Ester-Exchange Methods. *J. Chem. Soc. Resumed* **1962**, *1934*, 1934.
(37) Shen, Y.; Yang, X.; Song, Y.; Tran, D. K.; Wang, H.; Wilson, J.; Dong, M.; Vazquez, M.; Sun, G.; Wooley, K. L. Complexities of Regioselective Ring-Opening vs Transcarbonylation-Driven Structural Metamorphosis during Organocatalytic Polymerizations of Five-Membered Cyclic Carbonate Glucose Monomers. *JACS Au* **2022**, *2* (2), 515−521.
(38) Li, Y.; Wang, L.; Cao, Y.; Xu, S.; He, P.; Li, H.; Liu, H. Tris-Imidazolinium-Based Porous Poly(Ionic Liquid)s as an Efficient Catalyst for Decarboxylation of Cyclic Carbonate to Epoxide. *RSC Adv.* **2021**, *11* (23), 14193−14202.
(39) Fernandez Soraya, O. G., de Miranda, G., de Aberastui, J., Pérez, B., Madurga, M., Fernàndez, P. Glycidol Synthesis Method. WO 2017/017307 A1, 2016.
(40) Lukato, S.; Kasozi, G. N.; Naziriwo, B.; Tebandeke, E. Glycerol Carbonylation with CO2 to Form Glycerol Carbonate: A Review of Recent Developments and Challenges. *Curr. Res. Green Sustain. Chem.* **2021**, *4*, 100199.

https://doi.org/10.1021/acs.iecr.5c02554
Ind. Eng. Chem. Res. 2025, 64, 18630−18639

(41) Del-Mazo-Alvarado, O.; Prieto, C.; Sánchez, A.; Ramírez-Márquez, C.; Bonilla-Petriciolet, A.; Martín, M. An Integrated Process Analysis for Producing Glycerol Carbonate from CO_2 and Glycerol. *ChemSusChem* **2024**, *17* (8), No. e202301546.
(42) Sahani, S.; Upadhyay, S. N.; Sharma, Y. C. Critical Review on Production of Glycerol Carbonate from Byproduct Glycerol through Transesterification. *Ind. Eng. Chem. Res.* **2021**, *60* (1), 67−88.
(43) Zhang, H.; Li, H.; Wang, A.; Xu, C.; Yang, S. Progress of Catalytic Valorization of Bio-Glycerol with Urea into Glycerol Carbonate as a Monomer for Polymeric Materials. *Adv. Polym. Technol.* **2020**, *2020*, 7207068.
(44) Barzagli, F.; Mani, F.; Peruzzini, M. From Greenhouse Gas to Feedstock: Formation of Ammonium Carbamate from CO2 and NH3 in Organic Solvents and Its Catalytic Conversion into Urea under Mild Conditions. *Green Chem.* **2011**, *13* (5), 1267.
(45) Wang, H.; Xin, Z.; Li, Y. Synthesis of Ureas from CO2. *Top. Curr. Chem.* **2017**, *375* (2), 49.
(46) Fujita, S.; Yamanishi, Y.; Arai, M. Synthesis of Glycerol Carbonate from Glycerol and Urea Using Zinc-Containing Solid Catalysts: A Homogeneous Reaction. *J. Catal.* **2013**, *297*, 137−141.
(47) Zhang, L.; Zhang, Z.; Wu, C.; Qian, Q.; Ma, J.; Jiang, L.; Han, B. Microwave Assisted Synthesis of Glycerol Carbonate from Glycerol and Urea. *Pure Appl. Chem.* **2018**, *90* (1), 1−6.
(48) Romano, G.; Paradisi, E.; Rosa, R.; Leonelli, C.; Roncaglia, F. Synthesis of Glycerol Carbonate from Glycerol and Urea Using a Microwave Reactor. *AMPERE-Newsletter_111_OK*, 2022.
(49) Butburee, T.; Prasert, A.; Rungtaweevoranit, B.; Khemthong, P.; Mano, P.; Youngjan, S.; Phanthasri, J.; Namuangruk, S.; Faungnawakij, K.; Zhang, L.; Jin, P.; Liu, H.; Wang, F. Engineering Lewis-Acid Defects on ZnO Quantum Dots by Trace Transition-Metal Single Atoms for High Glycerol-to-Glycerol Carbonate Conversion. *Small* **2024**, *20* (44), 2403661.
(50) Deng, L.; Su, Q.; Ding, W.; Liu, S.; Li, Z.; Cheng, W. Anions Mediated Electron-Rich Metalloporphyrin Ionic Framework as Recyclable Catalyst for Conversion of Urea into Cyclic Carbonates. *J. Mol. Liq.* **2024**, *399*, 124468.
(51) Ab Rahim, M. H.; Zuhaimi, N. A. S.; Saud, A. S.; Madduluri, V. R.; Alshammari, H.; Maniam, G. P. Synthesis of Glycerol Carbonate from Industrial By-Products by Alcoholysis of Urea: Crude Glycerol and Red Gypsum. *Fuel* **2024**, *357*, 129774.
(52) Ptaszyńska, K.; Malaika, A.; Kozigrodzka, K.; Kozłowski, M. A Green Approach to Obtaining Glycerol Carbonate by Urea Glycerolysis Using Carbon-Supported Metal Oxide Catalysts. *Molecules* **2023**, *28* (18), 6534.
(53) Anderlini, B.; Ughetti, A.; Cristoni, E.; Forti, L.; Rigamonti, L.; Roncaglia, F. Upgrading of Biobased Glycerol to Glycerol Carbonate as a Tool to Reduce the CO2 Emissions of the Biodiesel Fuel Life Cycle. *Bioengineering* **2022**, *9* (12), 778.
(54) Ochterski, J. W. Thermochemistry in Gaussian, 2020. https://gaussian.com/wp-content/uploads/dl/thermo.pdf (accessed Aug 19, 2025).
(55) Chen, Z.; Li, Y.; He, Z.; Xu, Y.; Yu, W. Theoretical Investigations on Charge Transport Properties of Tetrabenzo[*a,d,j,m*]Coronene Derivatives Using Different Density Functional Theory Functionals (B3LYP, M06-2X, and wB97XD). *J. Chem. Res.* **2019**, *43* (7−8), 293−303.
(56) Schaber, P. M.; Colson, J.; Higgins, S.; Thielen, D.; Anspach, B.; Brauer, J. Thermal Decomposition (Pyrolysis) of Urea in an Open Reaction Vessel. *Thermochim. Acta* **2004**, *424* (1−2), 131−142.
(57) Nguyen-Phu, H.; Shin, E. W. Investigating Time-Dependent Zn Species over Zn-Based Catalysts in Glycerol Carbonylation with Urea and Their Roles in the Reaction Mechanism. *Appl. Catal. Gen.* **2018**, *561*, 28−40.
(58) Nguyen-Phu, H.; Shin, E. W. Disordered Structure of ZnAl2O4 Phase and the Formation of a Zn NCO Complex in ZnAl Mixed Oxide Catalysts for Glycerol Carbonylation with Urea. *J. Catal.* **2019**, *373*, 147−160.
(59) Andriyani, D. D.; Kadir, L. A.; Indriyani, N. P.; Permana, Y. Glycerol Carbonate Synthesis via Zn(OBu)2/AlCl2(OBu) Initiated-Glycerolysis of Urea. *Chem. Inorg. Mater.* **2024**, *2*, 100040.
(60) Turney, T. W.; Patti, A.; Gates, W.; Shaheen, U.; Kulasegaram, S. Formation of Glycerol Carbonate from Glycerol and Urea Catalysed by Metal Monoglycerolates. *Green Chem.* **2013**, *15* (7), 1925.

https://doi.org/10.1021/acs.iecr.5c02554
Ind. Eng. Chem. Res. 2025, 64, 18630−18639